Gu *et al. Journal of Ovarian Research* (2025) 18:65
https://doi.org/10.1186/s13048-025-01589-3

Journal of Ovarian Research

RESEARCH Open Access

Identification of exosome-related SERPINB1 as a novel predictor for tumor immune microenvironment and clinical outcomes in ovarian cancer

Rui Gu[1†], Liping Jiang[1†], Shuqin Dai[1], Yajie Yue[1], Shangjin Li[1], Shudan Zheng[1], Liwei Wu[1*] and Shaojie Zhao[1*]

Abstract

Background With a high global incidence of over three million new cases in 2020 and a high mortality of over two million fatalities, ovarian cancer is one of the most common malignant tumors in gynecology. Exosomes can control the immunological condition of the tumor microenvironment (TME) by participating in intercellular interactions. Therefore, we aimed to construct an exosome-related prognostic model to predict the clinical outcomes of ovarian cancer patients.

Methods In this research, expression patterns of exosome-related genes were examined in multiple single-cell RNA-sequencing and bulk RNA-sequencing datasets. In addition, a novel exosome-related prognostic model was established by the least absolute shrinkage and selection operator (LASSO) regression method. Then, the correlations between risk score and immunological characteristics of the TME were explored. Moreover, SERPINB1, a gene in the prognostic signature, was further analyzed to reveal its value as a novel biomarker.

Results In the current study, combined with single-cell and bulk omics datasets, we constructed an exosome-related prognostic model of four genes (LGALS3BP, SAT1, SERPINB1, and SH3BGRL3). Moreover, the risk score was associated with worse overall survival (OS) in ovarian cancer patients. Further analysis found that patients with high-risk score tended to shape a desert TME with hardly infiltration of immune cells. Then, SERPINB1, positively correlated with the favorable OS and negatively with the risk score, was chosen as the representative biomarker of the model. Moreover, SERPINB1 was positively correlated with the infiltration of immune subpopulations in both public and in-house cohort. In addition, the high-resolution analysis found that SERPINB1^{+} tumor cells communicated with microenvironment cells frequently, further explaining the potential reason for shaping an inflamed TME.

†Rui Gu and Liping Jiang contributed equally to this study.

*Correspondence:
Liwei Wu
fox2062@126.com
Shaojie Zhao
zsjie2005@163.com

Full list of author information is available at the end of the article

Conclusion To sum up, we established a novel exosome-related prognostic model (LGALS3BP, SAT1, SERPINB1, and SH3BGRL3) to predict the prognosis of patients with ovarian cancer and identify the immunological characteristics of the TME. In addition, SERPINB1 was identified as a promising biomarker for prognostic prediction in ovarian cancer.

Keywords Ovarian cancer, Exosome, Immune infiltration, SERPINB1, Gene signature

Background

Ovarian cancer is one of the most prevalent malignant tumors in the female reproductive system, with a high global incidence of over three million new cases in 2020 and a high mortality of over two million fatalities [1]. Statically, ovarian cancer patients, diagnosed at early stages have a five-year relative survival rate of more than 90%. However, more than two-thirds of ovarian cancer patients are diagnosed at advanced stages. Because most ovarian cancer patients are discovered at advanced stages of metastatic disease, uncontrolled proliferation of ovarian cancer cells is the fifth largest cause of cancer death in women [2, 3], despite innovative molecular targeted therapies [4]. Cytoreductive surgery combined with platinum chemotherapy is thought to be the best treatment for patients with advanced ovarian cancer [5]. However, most ovarian cancer patients who receive first-line platinum treatment develop platinum-resistant or platinum-refractory recurrent diseases [6].

Accumulating research on tumor ecosystems in numerous carcinomas has demonstrated the functional relevance of the tumor microenvironment (TME) in carcinogenesis and treatment responses [7]. TME refers to the tumor's non-cancerous cells and components, as well as the compounds produced or secreted by these cells. Exosomes are extracellular vesicles formed from endosomes that range in size from 30 to 150 nm and have an average diameter of 100 nm [8]. Exosomes released by tumor and TME cells serve critical roles in tumor cell-cell communication [9, 10]. Exosomal proteins can change the fate of exosome-releasing cells themselves via an autocrine pathway [11, 12]. For example, tumor-derived exosomes containing PD-L1 could attenuate the anti-tumor immunity and promote the immune escape of tumor cells with low- or no-expression of PD-L1 via transferring the PD-L1 expression [13]. Furthermore, tumor-derived exosomes (TEXs) can be taken up by immune and stromal cells that comprise the TME, modifying the TME infiltration pattern and influencing cell behavior [14, 15]. For instance, tumor-derived exosomes transferred tumor antigens heat-shock proteins (HSP70-80) and MHC-I molecules to DCs, which induced potent $CD8^{+}$T cell-dependent antitumor effects on mouse tumors [16, 17]. Besides, tumor-derived exosomes also block the differentiation of dendritic cell (DC) via downregulating MHC-II, but upregulating PD-L1 [18]. Therefore, because of the immune-activating and immune-suppressive functions of tumor-derive exosomes, understanding the exosome-related patterns should benefit efforts to target or utilize exosomes in cancer treatment.

Due to the unique message carried in them, their abundance in peripheral circulation, and the convenience of liquid biopsy [19, 20], exosomes had distinct advantages over other common cancer biomarkers. For instance, Sonia et al. identified glypican-1 specifically enriched in cancer-cell-derived exosomes, and then proved the potential role of it in non-invasive diagnostic and screening tools to detect early stages of pancreatic cancer [21]. Plasma exosomes contain CD63, a traditional exosome marker [22], and Cav1, a melanoma marker that were linked with a poor prognosis in melanoma [23]. However, due to these biomarkers are probably produced from both tumor cells and normal cells, exosomes derived from different bodily fluids of cancer patients are a diverse mix of vesicles [24]. To distinguish between cancer and normal origins, it is crucial to identify exosome markers.

In this study, a comprehensive bioinformatic analysis was performed on multi-omics data to identify the molecular features underlying the exosome-related prognostic signature. We first captured the up-regulated genes of tumor cells that had higher expressed levels of exosome-related genes at the single-cell levels. Subsequently, the weighted gene co-expressed network analysis (WGCNA) was performed to identify the exosome-related pattern in ovarian cancer patients. Then, a prognostic model was established based on the overlapping genes. The clinical relevance of the risk score, including therapeutic response and drug resistance, was also examined. Further analysis revealed the correlation between the risk score and immunological status. Overall, we reported an exosome-related prognostic model (LGALS3BP, SAT1, SERPINB1, and SH3BGRL3) to identify the immunological characteristics of the TME and predict clinical outcomes. In addition, SERPINB1 was identified as a promising biomarker for prognostic prediction in ovarian cancer.

Methods

Dataset acquisition

The normalized RNA-sequencing profiles and clinical information of ovarian cancer patients were downloaded from the UCSC Xena website (https://xenabrowser.net/datapages/) and the Gene Expression Omnibus (GEO) portal (https://www.ncbi.nlm.nih.gov/geo/). In the GEO database, we identified two cohorts (GSE9891 [25], and

GSE26712 [26]) with prognosis information. Samples with overall survival (OS) above zero day were included in this study (Table S1). In addition, the exosome-related genes were downloaded from Jiani Wu et al.'s study [27] and the ExoBCD database (https://exobcd.liumwei.org) [28] (Table S2).

Single-cell RNA sequencing datasets analysis

The single-cell RNA sequencing datasets of six patients with ovarian cancer from the GSE173682 dataset [29] were downloaded. All additional analyses were performed using the Seurat R toolkit (4.0.4, http://satijalab.org/seurat/) [30], including quality control and all subsequent analyses.

To reduce the impact of aberrant cells and technological background noise on downstream analysis, cells were reserved if mitochondrial gene expression was greater than 10%, or if identified genes were less than 200 or greater than 6,000. Next, the "RunHarmony" function in the R package harmony [31] was used to minimize the technical batch effects among individuals and experiments. The top 4,000 variable genes were used for principal component analysis (PCA) [32] to reduce dimensionality. The dimensionality of the scaled integrated data matrix was further reduced to two-dimensional space based on the first 30 principal components (PCs) and visualized by t-Distributed Stochastic Neighbor Embedding (t-SNE) [33]. The cell clusters were identified based on a shared nearest neighbor (SNN) [34] modularity optimization-based clustering algorithm with a resolution of 1. Then, these cells were annotated into different cell types based on the expression levels of conventional signatures, such as VWF for endothelial cells, EPCAM for epithelial cells, DCN for fibroblasts, CD3D for T cells, were used to verify the annotation of cell types.

Identification of up-regulated genes of tumor cells with high exosome score

The "PercentageFeatureSet" function was used to assess the expression of exosome-related genes in tumor cells obtained from public databases. Based on the median level, the tumor cells were classified into exosome-high and low groups. Then, the "FindAllMakers" function was performed to identify the up-regulated genes of each group (Table S2). Genes with avg_log2FC ≥ 0.25, pct.1 ≥ 0.5, and up-regulated in exosome-high groups were recognized as candidates.

Identification of exosome-related pattern of ovarian cancer patients

The single-sample gene sets enrichment analysis (ssGSEA) algorithm was utilized to calculate the enrichment scores of exosome-related genes of each ovarian cancer patients in the GSE9891 cohort. To explore the exosome-related pattern of ovarian cancer patients, we constructed a weighted co-expression network (WGCNA) according to the expression profile of the top 50% genes with highest variability (10, 822 genes) by utilizing the R package WGCNA [35] and then identified the significant gene modules positively related to levels of exosome scores.

The idea of a soft threshold is to continually elementize the elements in the Adjacency Matrix through a weight function and the choice of the soft threshold β is bound to affect the result of module identification. To create a network with a nearly scale-free topology, we installed the soft threshold power of $\beta = 3$ (scale-free $R^2 = 0.92$). Gene significance (GS) was defined as the correlation coefficient between gene expression and module traits. The module eigengene was calculated as a summary profile for each module. Module membership (MM) was defined by the correlation coefficient of the module eigengene and gene expression profile. Genes with GS ≥ 0 and MM ≥ 0 in modules highly associated with exosome scores were identified as the exosome-related pattern of ovarian cancer patients and extracted for further study.

Construction of the prognostic model

Next, exosome-related prognostic model were constructed based on the overlapping genes of exosome-related candidates identified at the single-cell and bulk omics levels. Univariable COX regression analysis was performed to screen genes that were significantly associated with overall survival (P-value < 0.1). Subsequently, the least absolute shrinkage and selection operator (LASSO) regression method was used to find out the potential prognostic gene sets, which were defined as exosome biomarkers. The risk score of the prognostic model based on exosome biomarkers in patients was calculated based on the linear combination of the expression values of exosome biomarkers multiplied by the corresponding LASSO coefficients. To confirm the role of the risk score in the prediction of prognosis, we divided the patients into high- and low-risk score groups with a 50% cutoff according to the risk scores.

Assessment of immunological characteristics of the tumor microenvironment

In order to assess the immunological characteristics of the TME, the ESTIMATE algorithm [36], a method inferring tumor purity and stromal and immune cell from tumor samples based on bulk transcriptomic profile, was performed to assess tumor purity, ESTIMATE score, immune score, and stromal score. Besides, the information of immunomodulators including MHC signatures, receptors, chemokines, and immune stimulators was collected from the a previous study [37]. To further deconstruct the immunological status of each patient, a set of

signature genes of 29 immune cell types and immune-related pathways [38] was used to estimate the infiltration levels of different immune cell populations and the activities of immune-related pathways and functions of each patient were calculated by utilizing the ssGSEA algorithm in the R package "GSVA" [39].

Functional and pathway enrichment analyses

Gene annotation enrichment analysis was conducted using the "clusterProfiler" package [40]. Gene Ontology (GO) [41] terms were identified with a strict cutoff of p-value < 0.05.

Immunohistochemistry and semi-quantitative analysis

Ovarian tumor microarray (TMA) HOvaC063PT01, which was purchased from Outdo BioTech, contained 63 ovarian cancer samples. The use of the TMA was approved by the Clinical Research Ethics Committee in Outdo Biotech (Shanghai, China). The TMA was submitted for immunohistochemistry (IHC) assay to examine the expression of SERPINB1 protein in tumor and para-tumor tissues. The primary antibody utilized in the study was anti-SERPINB1 (1:200 dilution, Cat. AFW6257, Afantibody) and anti-CD8 (ready-to-use, Cat. PA577, Abcarta). Antibody staining was visualized with DAB and hematoxylin counterstain. Stained TMA was evaluated to define CD47 expression by two independent senior pathologists according to the immunoreactivity score (IRS) standard [42]. For the assessment of tumor-infiltrating $CD8^+$ T cells, two senior pathologists estimated the CD8 score according to the criterion established by The Cancer Genome Atlas Network [43]. A CD8 score defined as the sum of the distribution and density scores (0–6) was calculated for each case. Samples with the CD8 score ≥ 3 (3, 4, 5, 6) are considered immune-enrich, and samples with the CD8 score ≤ 2 (0, 2) are considered immune-desert.

Isolation and identification of exosomesWhen reached 50–60% confluency, SKOV3 cells (Cat. KGG3233-1, KeyGEN) and SKOV3 cells treated with recombinant SERPINB1 protein (100ng/mL, Cat. HY-P71303, MedChemExpress) were washed with PBS twice and incubated with McCoy's 5 A containing 10% exosome-depleted FBS (prepared by 16 h overnight ultracentrifugation at 120,000×g at 4 °C) for 48 h. Exosomes were isolated from the conditioned medium by ultracentrifugation [44]. The concentration of the exosomes were quantified by BCA (Beyotime, Shanghai, China) and exosomes were ready for cell treatment. For the identification of exosomes, exosome pellets, dissolved in PBS buffer were dropped in a carbon-coated copper grid and then stained with 1% uranyl acetate. The samples were observed using a transmission electron microscope. Nanoparticles in exosome suspensions were analyzed using a Flow Nanoanalyzer. In addition, exosomes were lysed using a radioimmunoprecipitation assay lysis buffer supplemented with PMSF inhibitor. Protein lysates were loaded and separated on a 10% sodium dodecyl sulfate polyacrylamide gel and transferred onto 0.22-μm polyvinylidene fluoride membranes. Primary antibodies against TSG101 (Cat. 28283-1-AP, ProteinTech) and CD63 (Cat. 25682-1-AP, ProteinTech) were used.

In vitro cytotoxicity assay

Peripheral blood monouclear cells (PBMC) were collected from healthy controlS. The CD8 + T cells were isolated using Dynabeads human CD8 selection Kit (catalog 11333D, Invitrogen) and cultured in ImmunoCult-XF T cell expansion medium (catalog 10981, STEMCELL Technologies). ImmunoCult human CD3/CD28 T cell activator (catalog 10971, STEMCELL Technologies) was used to activate T cells, and then T cells were treated with exosomes (10 μg/mL) isolated from SKOV3 cells and SKOV3 cells treated with recombinant SERPINB1 protein at 37 °C for 48 h. T cells were submitted for flow cytometry analysis to detect the activated marker CD69.

Statistical analysis

All statistical analyses were handled using R software (version 4.0.4). The significant difference in continuous variables between the two groups was assessed using the Wilcoxon rank-sum test, while the fisher exact test was used to measure the difference among categorical variables. For all analyses, a two-paired p-value < 0.05 was deemed to be statistically significant, and labeled with *p-value < 0.05, **p-value < 0.01, ***p-value < 0.001, and ****p-value < 0.0001.

Results

Exosome-related genes expressed specifically in ovarian cancer cells at single-cell atlas.

In order to characterize the exosome-related genes of ovarian cancer at the single-cell level, we collected the scRNA-seq datasets from six ovarian cancer patients (Fig. 1A). After quality control, unsupervised clustering, and cell annotation, a total of 32.129 individual cells from the six ovarian cancer patients were classified into six major cell types based on the expression levels of conventional biomarkers (Fig. 1A-D). The specifically expressed genes of each cell type were identified to further verify the annotation of single cell (Fig. 1E). Subsequently, we estimated the exosome scores of individual cells based on the expressed fractions of exosome-related genes. Results showed that compared with non-tumor cells, tumor cells had higher levels of exosome-related genes collected from public databases (Fig. 1F). Then, the tumor cells were divided into exosome-high and low groups based on the median value of exosome scores. Next, we

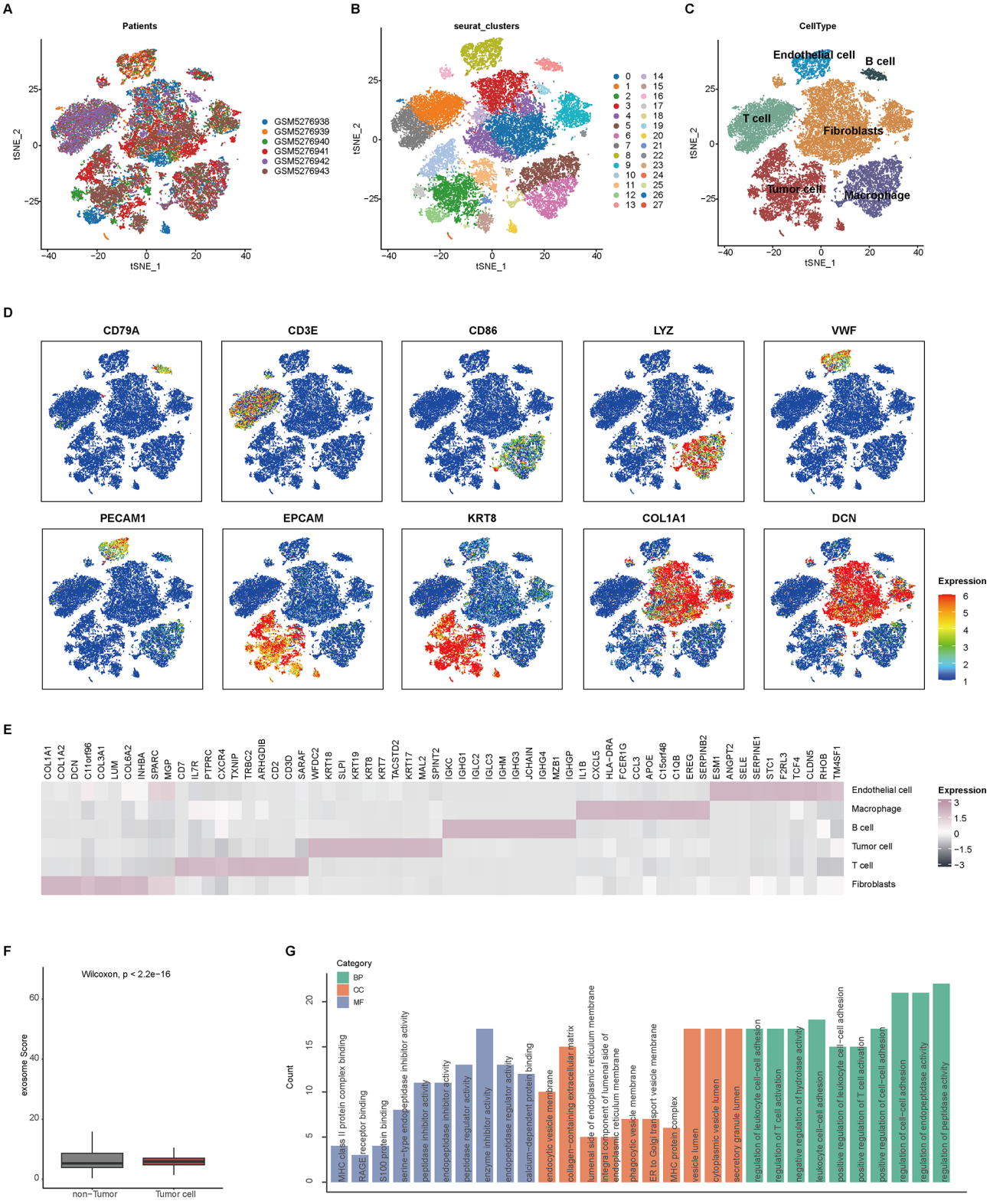

Fig. 1 Integrated scRNA-seq analysis of tumor tissues from ovarian cancer patients. (**A**) t-SNE visualization of 32,129 single cells passed quality controls, colored by six ovarian cancer patients. (**B**) The unsupervised clustering of 32,129 cells. (**C**) t-SNE visualization of cell types annotated by classical gene markers. (**D**) Expression levels of known markers for specific cell types overlaid on the t-SNE representation. (**E**) Heatmap for gene expression levels of top ten cell-type-specific genes. (**F**) Comparing the exosome scores between tumor and non-tumor cells. (**G**) Bar plot showing the enriched signaling pathways in tumor cells with high exosome scores

investigated the biological process of tumor cells with exosome-high phenotype in ovarian cancer patients. Results showed that tumor cells with exosome-high phenotype significantly up-regulated some signaling pathways which can be mediated by exosomes, such as S100 protein binding [45, 46] (Fig. 1G), suggesting that tumor cells may have higher levels of exosome-related genes, and exosome is an important feature of tumor cells.

Exploration of exosome-related patterns of ovarian cancer patients

Given of the important functional role of TME in mediating the activities of cells and exosomes, we then explored the exosome-related pattern of ovarian cancer patients at the bulk omics levels. The GSE9891 cohort was utilized for this part. Based on the enrichment scores of exosome-related genes, the WGCNA algorithm was used to identify the notable gene modules that were positively connected with the levels of exosome-related genes. The soft threshold power was set to = 3 (scale-free $R^2 = 0.92$, Fig. 2A-B). Next, 28 color-coded gene modules except for the gray module were held for further research (Fig. 2C). As shown in Fig. 2D, the turquoise module had the highest correlation with exosome scores ($R = 0.48$, $P < 0.0001$). The GS and MM values for the turquoise module in exosome scores were displayed in scatter plots (Fig. 2E). Genes with gene significance (GS) > 0 and module membership (MM) > 0 in modules highly associated with the exosome scores were identified as exosome-related patterns of ovarian cancer patients, and then extracted for further study. Further analysis showed that these genes were associated with the enrichment of some signaling pathways reflecting the activities of exosomes, such as CCR chemokine receptor binding [47] and cytokine binding [48, 49].

Construction and validation of exosome-related prognostic signature

Based on exosome-related genes identified at the single-cell and bulk omics levels, a total of 45 overlapping genes of them were used for further analysis (Fig. 3A). To choose genes with prognostic values, univariable COX regression analysis of these selected genes correlated with OS in ovarian cancer was performed (Table S4). Then, LASSO COX analysis was applied to further reduce the scale of independent prognostic genes to four genes (LGALS3BP, SAT1, SERPINB1, and SH3BGRL3) (Fig. 3B-C). The expression of LGALS3BP, SAT1, and SERPINB1 behaved with favorable prognosis prediction ability, while SH3BGRL3 was the opposite (Fig. 3C and Figure S1).

Next, a prognostic model of the four genes was constructed. The risk scores of patients were calculated according to the combination of the expression levels of these genes multiplied by the corresponding coefficients. The risk scores of ovarian cancer patients in the GSE9891 cohort were further shown in Fig. 3D. The death cases were focused in the high-risk score group, and the surviving cases were centralized in the low-risk score group (Fig. 3D). Besides, patients with high risk score showed a worse prognosis, compared with patients with low risk score (Fig. 3E). In addition, patients with higher pathological stages or grades had higher levels of risk scores (Fig. 3F-H), which further supported the finding that patients with high-risk score had worse clinical outcomes than those with low-risk score. The prognostic prediction of the model was validated in other independent cohorts. Consistently, patients in the high-risk score group showed worse prognosis (Fig. 3I-K).

Ovarian cancer patients with high-risk score exhibited a dessert TME

Given that the important role of TME in clinical outcomes and therapeutic responses, we next investigated the biological characteristics of high- and low- risk score groups. Results showed that patients in the low-risk score groups had higher activation of immune-related pathways, such as positive regulation of T cell activation, positive regulation of leukocyte cell-cell adhesion, and Cytokine-cytokine receptor interaction, while some signaling pathways associated with cell proliferation were enriched in patients with high-risk score phenotype (Fig. 4A-B). Additionally, ovarian cancer patients in the low-risk score group had higher levels of StromalScore, ImmuneScore, ESTIMATEScore, but lower tumor purity (Fig. 4C), suggesting that ovarian cancer patients in the low-risk score tended to shape an inflamed TME. Subsequent analysis further supported the hypothesis. Patients with low-risk core had higher levels of conventional biomarkers of immune subpopulations, such as GZMA, and GZMB, which were associated with the activation and cytotoxic with T cells (Fig. 4D) [50]. In addition, we further assessed the immunological status of TME based on the signature biomarkers of 29 immune cell types and immune-related pathways. Results showed that the risk scores were negatively correlated with almost all immunological characteristics (Fig. 4E), and the low-risk score group had higher enrichment scores of these immunological characteristics (Figure S2A). Also, ovarian cancer patients with higher risk scores showed lower levels of anti-tumor cycles (Fig. 4F and Figure S2B), suggesting that the low-risk score group exhibited the dessert TME feature, but those with high-risk score phenotype shaped an inflamed TME with more activated immune status.

Given that the limitation of the GSE9891 cohort, the TCGA cohort was included in our study to further support these results. Consistently, in the TCGA cohort, some signaling pathways associated with immunological

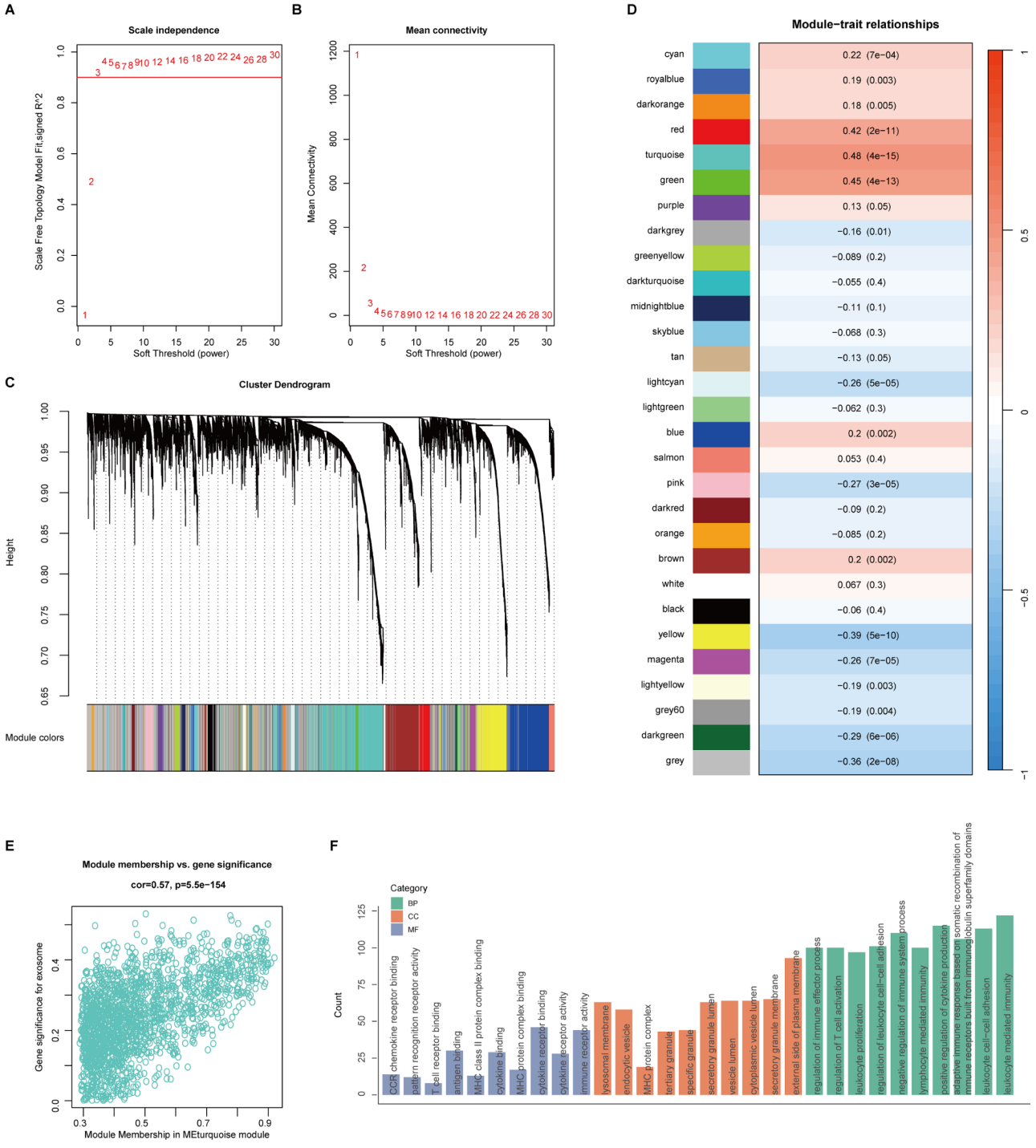

Fig. 2 Identification of exosome-related patterns in the GSE9891 cohort. (**A**) Analysis of the scale-free fitting indices for different soft-thresholding powers (β). (**B**) Mean connectivity analysis of different soft-thresholding powers. (**C**) Clustering dendrograms of genes were based on dissimilarity topological overlap and module colours. As a result, 28 co-expressed modules except grey module were constructed and labeled with different colours. These modules were arranged from large to small according to the number of genes included. (**D**) Heatmap of the correlation between module eigengenes and exosome scores of ovarian cancer. The turquoise gene module was revealed to exhibit the highest correlation with exosome score. (**E**) Scatter plots showing the relationship between MM and GS in the turquoise module. (**F**) GO analyses of genes in the turquoise module

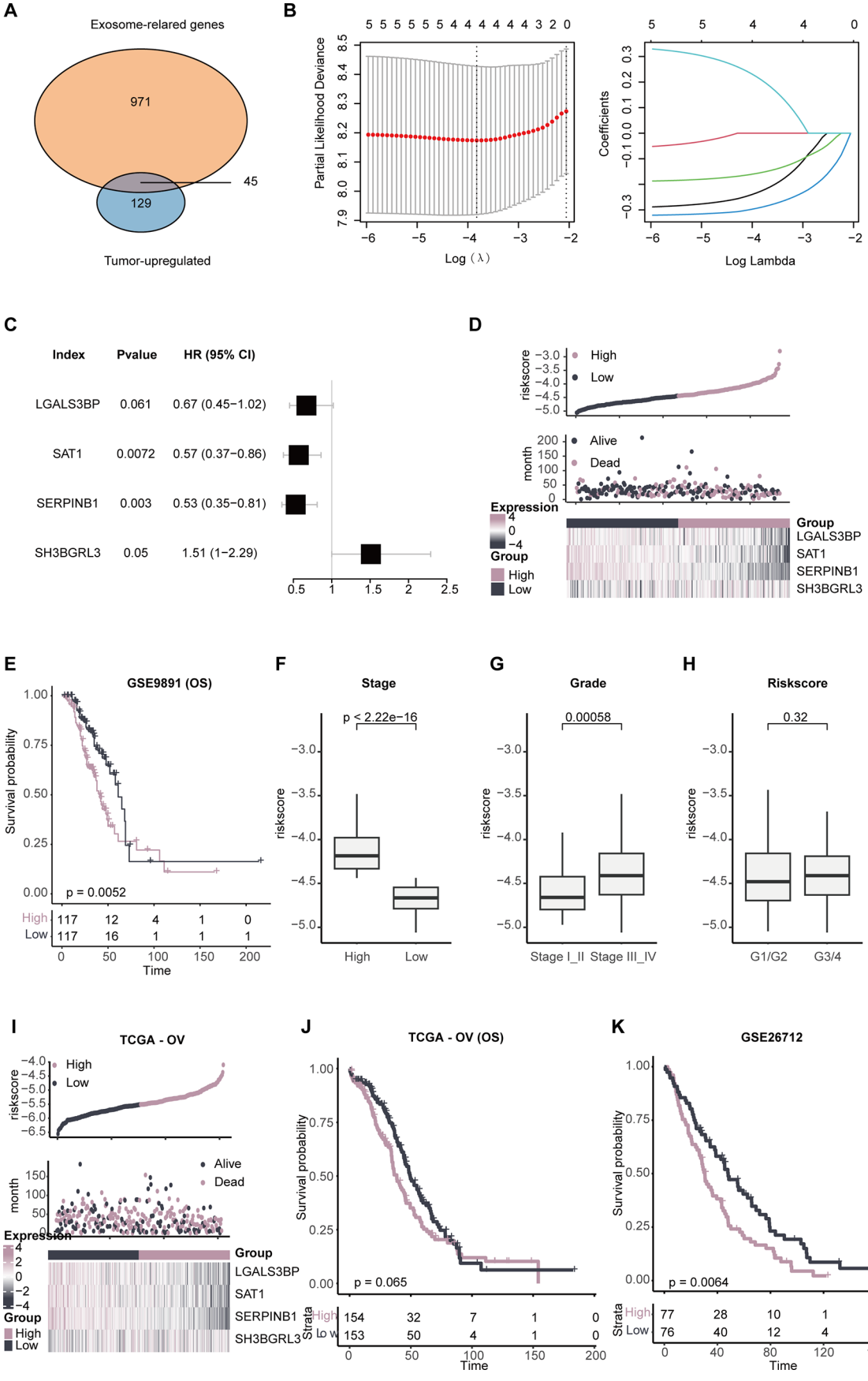

Fig. 3 (See legend on next page.)

(See figure on previous page.)

Fig. 3 Construction of exosome-related prognostic model in the GSE9891 cohort. (**A**) Venn diagram of overlapping genes in tumor cell-upregulated genes identified in the scRNA-seq datasets and the exosome-related genes identified by WGCNA. (**B**) The LASSO coefficient profiles were constructed using exosome-related genes, and the tuning parameter (λ) was calculated based on the minimum criteria for OS with ten-fold cross validation. Four genes were selected according to the best fit profile. (**C**) Univariable analyses of the expression values of the four genes with overall survival in GSE9891. (**D**) Distributions of CAFRS, survival status of ovarian cancer patients, and expression profiles of the gene signatures in the GSE9891 cohort. (**E**) Survival analysis showing the prognostic value of CAFRS in the GSE9891 cohort. (**F**-**H**) Comparing the risk score between patients with different clinic-pathological features. (**I**) Distributions of risk score, survival status of ovarian cancer patients, and expression profiles of the gene signatures in the TCGA cohort. (**J**-**K**) Survival analysis showing the prognostic value of CAFRS in the TCGA (J) and the GSE26712 cohort

activities were enriched in the patients with low-risk score phenotype (Fig. 5A-B). Also, almost all 29 immune cell types and immune-related pathways were up-regulated in the low-risk score group (Fig. 5C and Figure S3A). Additionally, the low-risk score group had higher levels of well-established biomarkers of immune subpopulations and immunomodulatory factors (MHC signatures, receptors, chemokine, immune stimulators) (Fig. 5D-E, and Figure S3B), suggesting that patients with the low-risk score phenotype had an immune infiltration TME, but the high-risk score group shaped a dessert TME.

In keeping with the results found in the GSE9891 and the TCGA cohorts, patients in the GSE26712 showed the similar results. Some immune-related signaling pathways were enriched in the low-risk score group (Figure S4A). Also, patients with the low-risk score phenotype had higher levels of immunological characteristics, including the immunomodulatory factors, immune-related pathways, and the anti-tumor cycles (Figure S4B-E). Totally, all these results suggested that the exosome-related prognostic model could reflect the immunological status of ovarian cancer patients, and be negatively associated with the formation of an inflamed TME.

SERPINB1 was a TEX biomarker for ovarian cancer

Next, we chose the representative gene of the prognostic model. Firstly, we compared the transcriptional level and the expressed fraction of four genes at the single-cell levels. Compared with other genes, tumor cells had obviously higher levels of SERPINB1 (Fig. 6A-D and Figure S5A-B). Also, tumor cells had the highest expressed fraction of SERPINB1 than other genes (Fig. 6A-D and Figure S5A-B). Considering the correlation between risk score and immunological characteristics, we further compared the correlation between gene expression and Immune Scores. Results showed that SERPINB1 had the largest correlation with Immune Scores in the GSE9891 cohort ($R = 0.45$, $p < 0.0001$, Fig. 6E-F, and Figure S5C-D). Also, in other independent cohorts, SERPINB1 expression showed the highest correlation with Immune Score (TCGA: $R = 0.48$, $p < 0.0001$; GSE26712: $R = 0.53$, $p < 0.0001$, Figure S6 and S7). In addition, we also used an ovarian cancer cohort to validation the positive correlation between SERPINB1 and CD8. The results showed that SERPINB1 was positively correlated with CD8 expression and highly expressed in the immune-enrich group (Fig. 7A and C). Moreover, we isolated exosomes from SKOV3 cells and SKOV3 cells treated with recombinant SERPINB1 protein (Fig. 7D-F), then added these exsoomes into T cells culture medium. The results showed that exosomes from SKOV3 cells treated with recombinant SERPINB1 protein could increase the activated level of T cells (Fig. 7G). Combined with these findings, SERPINB1 was chosen as the TEX biomarker of ovarian cancer patients, which was related to the activated TME features.

SERPINB1+ tumor cells communicated with immune subpopulations frequently

Having observed that the expression of SERPINB1 was positively correlated with the immunological characteristics (Fig. 5C, Figure S6C and Figure S7C), we next sought to investigate the reasons why patients with high SERPINB1 tended to shape an inflamed TME. Benefiting from the advantages of scRNA-seq technology, we could perform a high-resolution dissection of interactions among various subgroups of $SERPINB1^{+/-}$ tumor cells and microenvironment subpopulation in the ovarian cancer patients based on the combining expression of multi-subunit ligand-receptor complexes. The number of interactions among different subpopulations was compared between $SERPINB1^{+}$ and $SERPINB1^{-}$ tumor cells. Results showed that the $SERPINB1^{+}$ tumor cells presented significantly more interactions than $SERPINB1^{-}$ tumor cells (Fig. 8A and B). Notably, we calculated the difference in interaction numbers among various $SERPINB1^{+/-}$ tumor cells and microenvironment subpopulations. The $SERPINB1^{+}$ tumor cells showed more frequent crosstalk with other subpopulations (Fig. 8B), suggesting that compared with $SERPINB1^{-}$ tumor cells, $SERPINB1^{+}$ tumor cells had activated cell-cell communications, especially interactions with immune cells, which potentially take part in the formation of an immunosuppressive TME [51].

Using the CellphoneDB tool, we further discovered the important ligand-receptor interactions between $SERPINB1^{+}$ tumor cells and immunological subsets (Fig. 8C and D). Results revealed that ICOSLG-ICOS and PVR-TIGIT, which have been implicated in the suppression of the anti-tumor response [52–55], were the communication pathways used by $SERPINB1^{+}$ tumor cells to interact

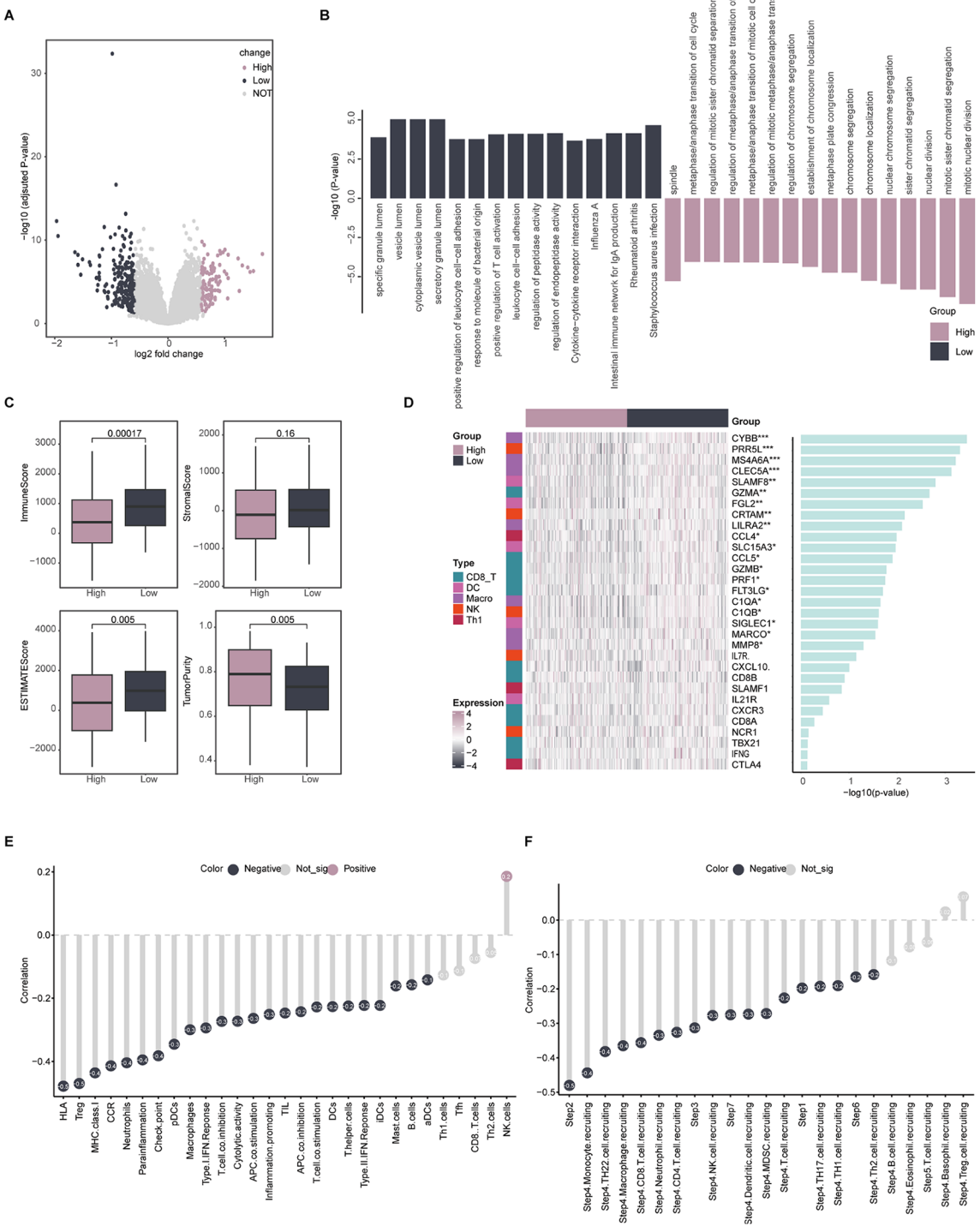

Fig. 4 Immunological characteristics between low-risk score and high-risk score groups in the GSE9891 cohort. (**A**) DEG analysis between the high- and low- risk score groups. (**B**) Pathway enrichment analyses of genes up-regulated in the high- and low-risk score groups, respectively. (**C**) Comparing the StromalScore, ImmuneScore, ESTIMATEScore, and tumor purity between high- and low-risk score in the GSE9891 cohort. (**D**) Heatmap showing the expression levels of conventional biomarkers of immune subpopulations. (**E**) The correlation between risk score and the enrichment scores of immune subpopulations and immune-related signaling pathways in the GSE9891 cohort. (**F**) The correlation between risk score and the enrichment scores of anti-tumor cycles in the GSE9891 cohort

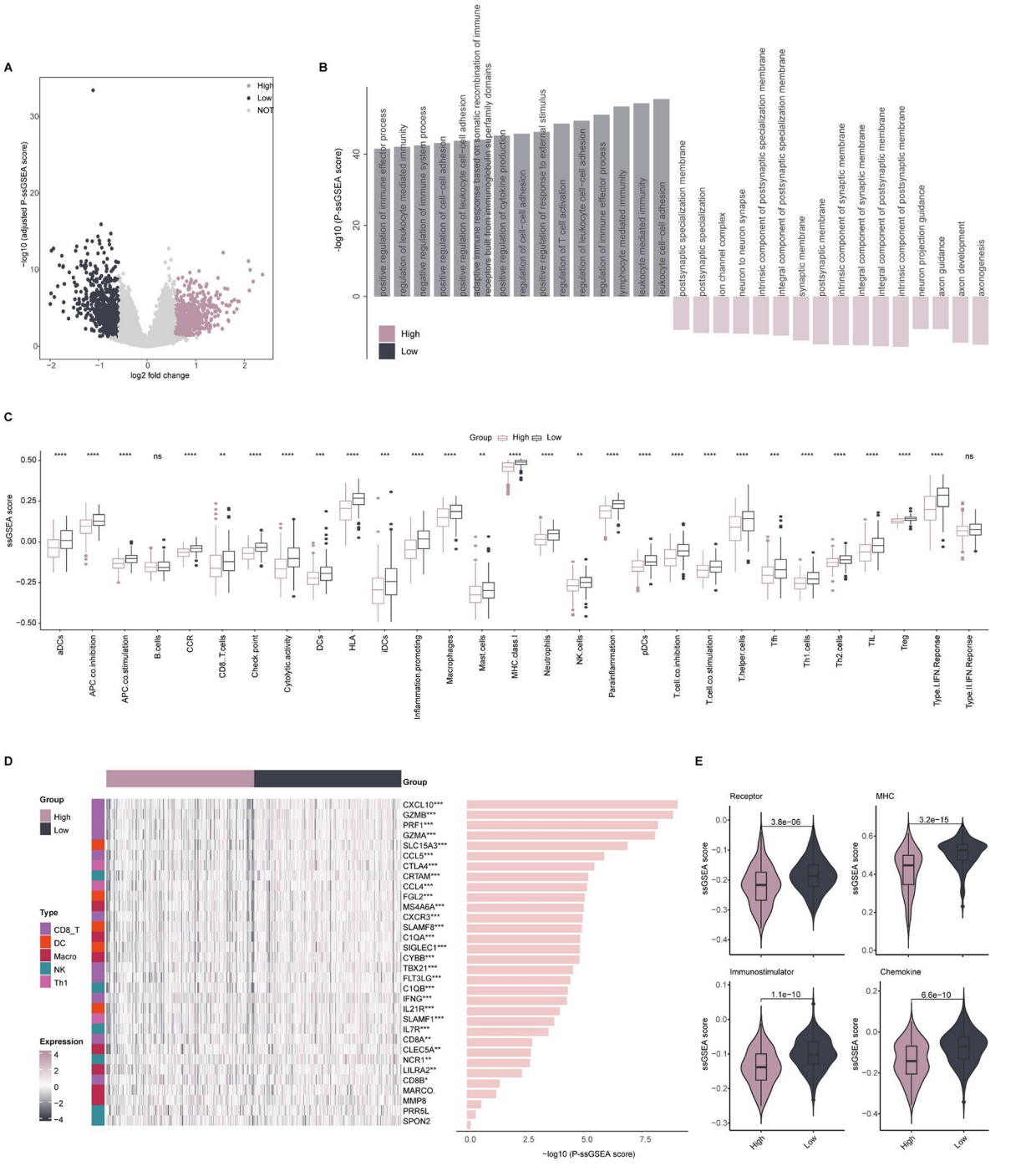

Fig. 5 Immunological characteristics between low-risk score and high-risk score groups in the TCGA cohort. (**A**) DEG analysis between the high- and low- risk score groups. (**B**) Pathway enrichment analyses of genes up-regulated in the high- and low-risk score groups, respectively. (**C**) Comparing the enrichment scores of immune subpopulations and immune-related signaling pathways between high- and low-risk score groups. (**D**) Heatmap showing the expression levels of conventional biomarkers of immune subpopulations. (**E**) Comparing the enrichment scores of receptor, MHC moleculars, Immunostimulator, and Chemokine between high- and low-risk score group

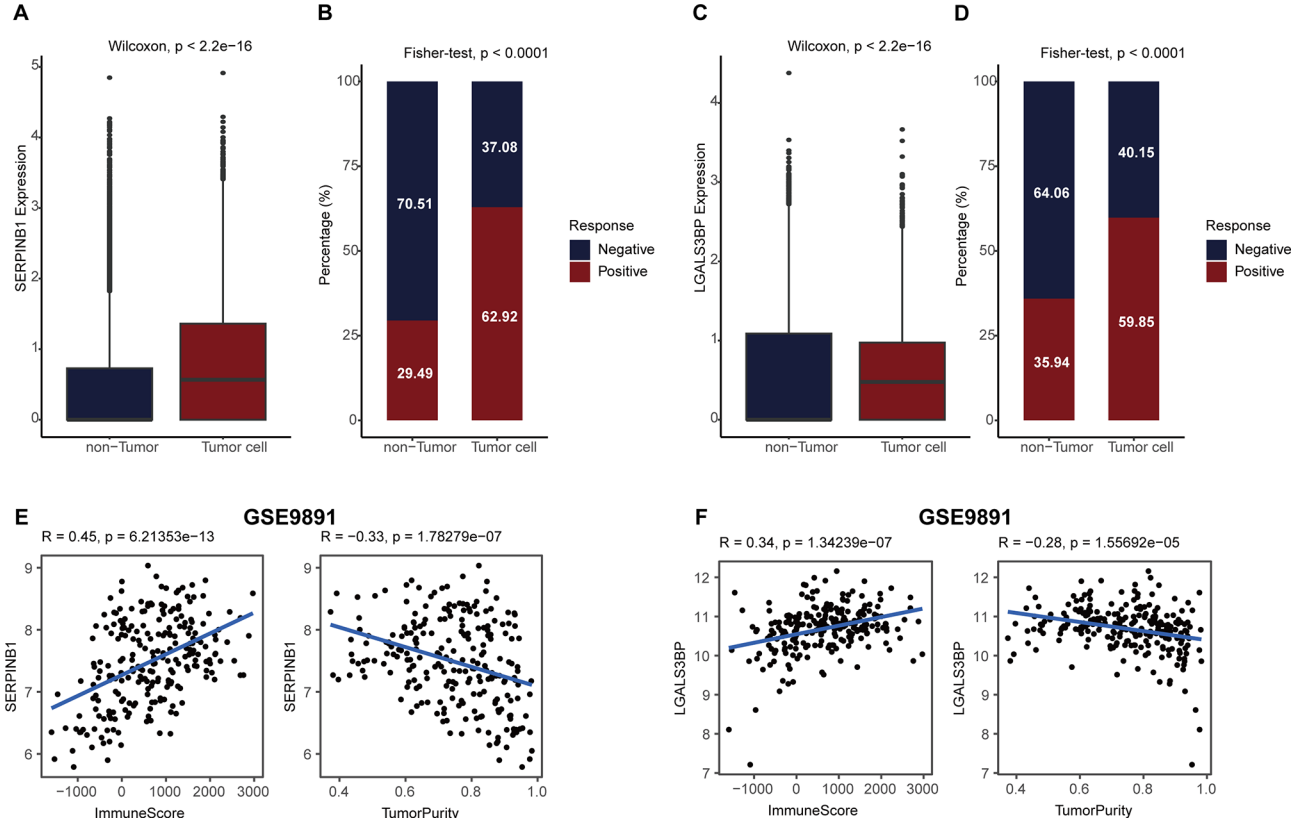

Fig. 6 SERPINB1 was a TEX biomarker for ovarian cancer. (**A**) Comparing the SERPINB1 expression between tumor and non-tumor cells. (**B**) Stacking bar chart showing the expressed fraction of SERPINB1 between tumor and non-tumor cells. (**C**) Comparing the LGALS3BP expression between tumor and non-tumor cells. (**D**) Stacking bar chart showing the expressed fraction of LGALS3BP between tumor and non-tumor cells. (**E**) Correlation between SERPINB1 expression and ImmuneScore and tumor purity in the GSE9891 cohort. (**F**) Correlation between LGALS3BP expression and ImmuneScore and tumor purity in the GSE9891 cohort

with myeloid cells. Additionally, ANXA1-FPR1 and other inhibitory ligand-receptor pairings were used by the SERPINB1$^+$ tumor cells to mediate the malfunction of T cells [56, 57]. The fact that SERPINB1$^+$ tumor cells interacted with immune subpopulations more frequently suggests that ovarian cancer patients with significant SERPINB1$^+$ tumor cell counts may have more complex TMEs and mediate the TME's immunological status.

Discussion

Ovarian cancer is a lethal malignancy in gynaecological diseases and is a complex disease, with a high global incidence of over three million new cases in 2020 and a high mortality of over two million fatalities [1]. Although the five-year relative survival rate of early-diagnosed ovarian cancer patients was over 90%, considerable ovarian cancer patients were diagnosed at an advanced stage and had worse clinical outcomes [4]. Cytoreductive surgery combined with platinum chemotherapy is thought to be the best treatment for patients with advanced ovarian cancer [5]. However, most patients with ovarian cancer who receive first-line platinum treatment develop platinum-resistant or platinum-refractory recurrent ovarian cancer [6].

With the in-depth research of tumor ecosystem, the tumors can be recognized as immune-hot and cold according to their cellular compositions and immunological status [58, 59]. Accumulating evidence has proved that targeting or reprograming the immunological status of TME can influence therapeutic responses. Exosomes have recently received a lot of attention in research because of the various ways in which they mediate the microenvironment in both healthy and pathological settings by transferring proteins, nucleic acids, and lipids [9, 10]. Owing to the heterogeneity of cancer cells, exosomes or EVs derived from host cancer cells can activate the receptors or modify the transcriptional expression in the neighboring cancer cells to alter their biological characteristics. For instance, breast cancer cells released exosomes harboring PD-L1, allowing its transfer to other cancer cells expressing low- or no- PD-L1, promoting tumor immune evasion [13]. Endometrial cancer cells secreted the exosomal LGALS3BP, and then triggered the PI3K/AKT/VEGFA signaling pathway to promote the proliferation and migration of endometrial cancer

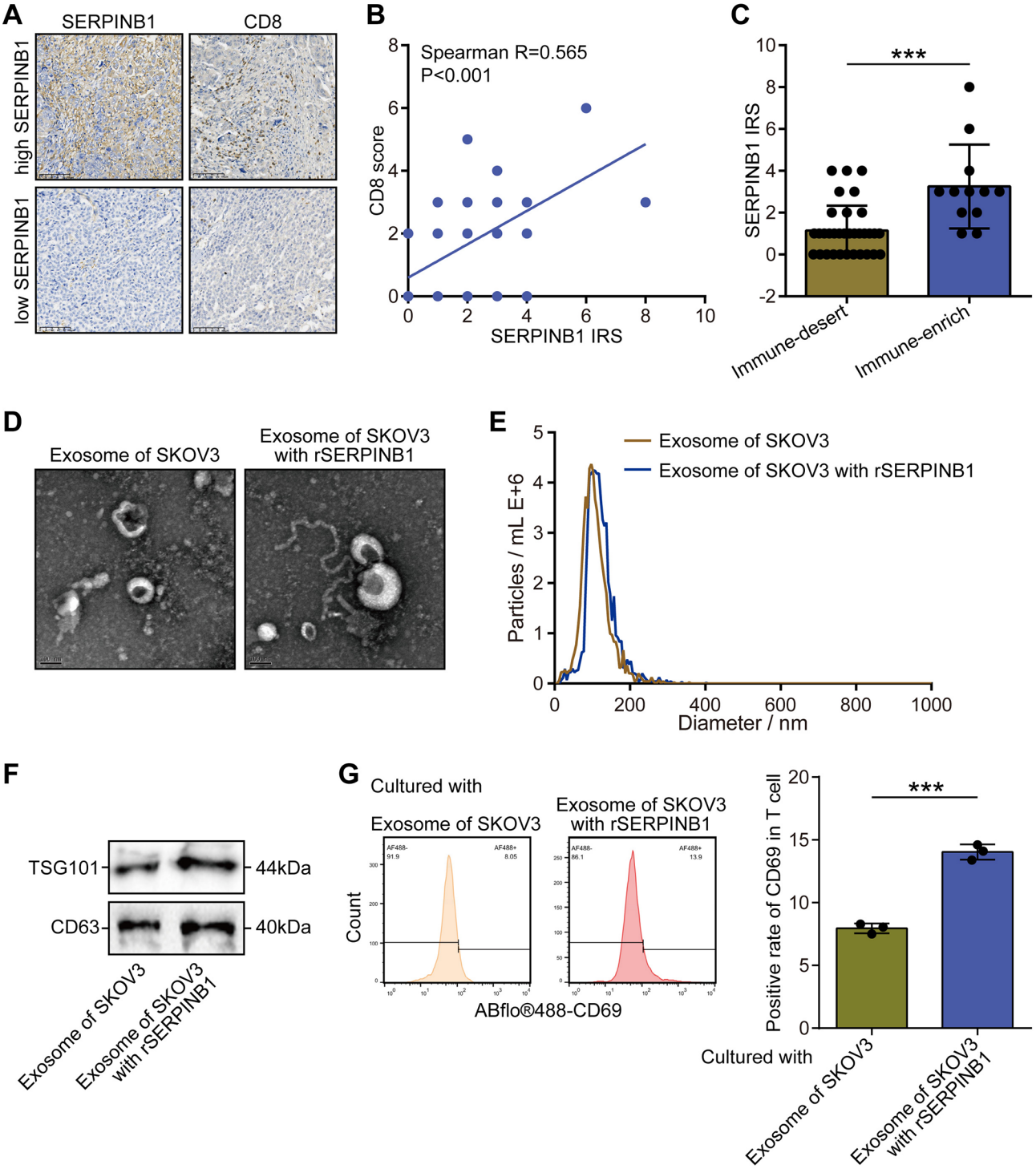

Fig. 7 Validation of the regulatory role of SERPINB1 in CD8 + T cells functions. (**A**) Representative images uncovering the expression of SERPINB1 and CD8 in ovarian cancer tumor tissues. (**B**) Correlation between SERPINB1 expression and CD8 score in ovarian cancer. (**C**) Differential expression of SERPINB1 in immune-desert and immune-enrich tumor samples. ***$P < 0.001$. (**D**) Transmission electron microscopy. Transmission electron micrographs of purified exosomes secreted from SKOV3 cells and SKOV3 cells treated with recombinant SERPINB1 protein. Scale bar, 100 nm. (**E**) Nanoparticle analysis. Concentration and size distribution of nano-sized particles in exosome suspension. (**F**) Western blot analysis of exosomes isolated from SKOV3 cells and SKOV3 cells treated with recombinant SERPINB1. (**G**) Activation levels of T cells treated with exosomes isolated from SKOV3 cells and SKOV3 cells treated with recombinant SERPINB1 protein

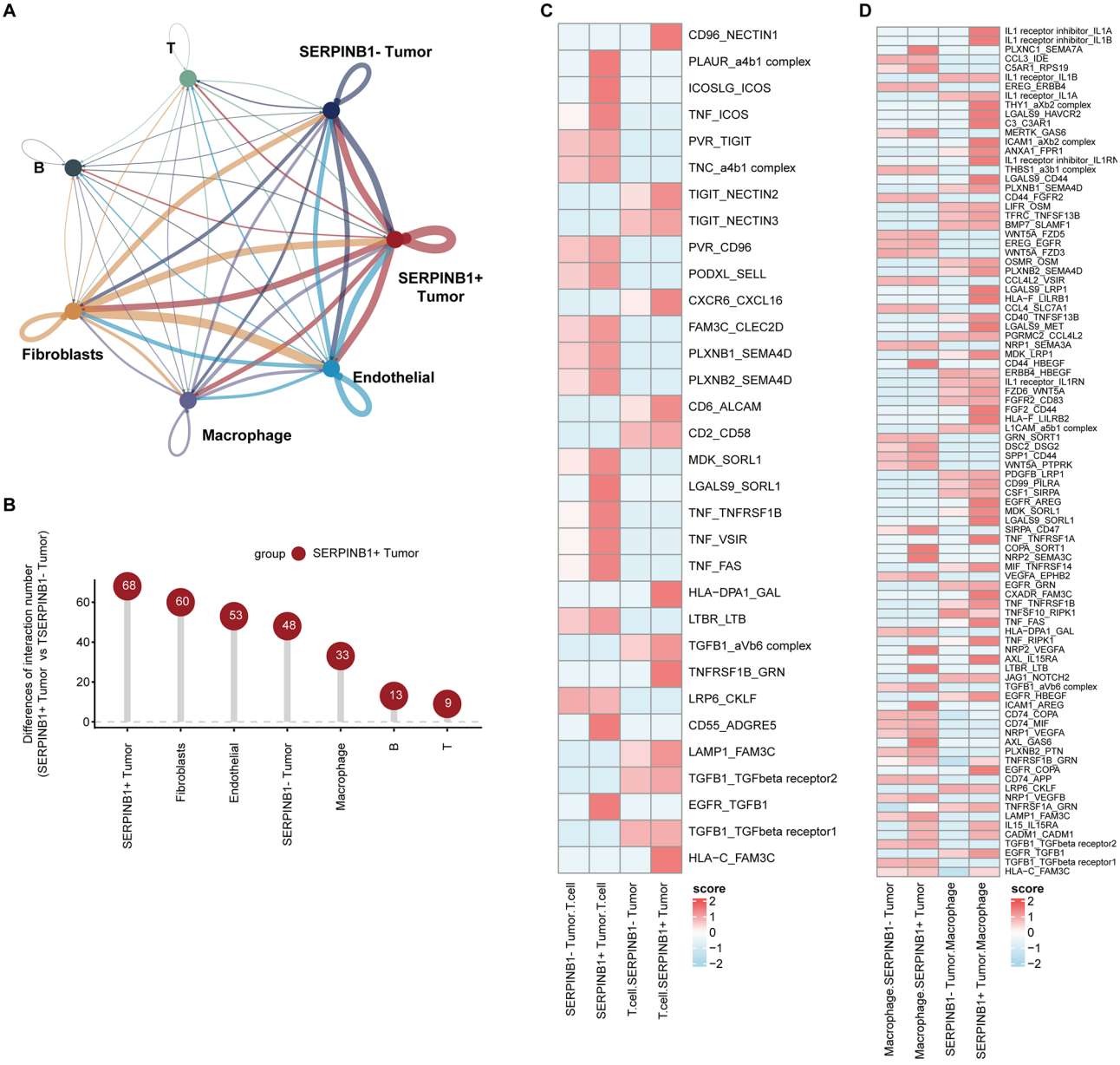

Fig. 8 Cell-cell communications between SERPINB1+/- tumor cells and microenvironment subpopulations. (**A**) The interaction number of SERPINB1+/- tumor cells and microenvironment subpopulations. The thickness of the line represents the interaction number between the subpopulations estimated by the CellPhoneDB tool. (**B**) The difference of the number of ligand-receptor interactions between SERPINB1 + and SERPINB1- tumor cells. (**D**) The inhibitory interactions between SERPINB1 + tumor cells and myeloid cells. (**E**) The inhibitory interactions between SERPINB1 + tumor cells and T cells

cells in vitro and vivo [60]. Similarly, mutant KRAS, along with other oncogenes such as EGFR and SRC, can be transferred by exosomes to recipient colon cancer cells of wild-type KRAS, promoting tumor invasion [61]. Additionally, TEXs could affect the TME, which is comprised of immunological and stromal cells, thus altering the TME's pattern of infiltration and impacting cell activity [62]. The tumor-derived exosomes present neo-antigens and/or MHC-peptide complexes to prime and activate T cells by direct presentation and cross-presentation through DCs, or directly activate NK cells or macrophages [16, 63, 64]. On the contrary, tumor-derived exosomes also can contribute to the immunosuppressive TME by inhibiting functions of NK and T cells, blocking DC differentiation, recruiting myeloid-derived suppressor cells (MDSCs) [65, 66] and stimulating the M2 polarization of macrophages [67]. Therefore, due to the double-planedness of exosomes, understanding the exosome-related pattern of ovarian cancer patients can reflect the immunological status of TME and guide clinical treatment.

Therefore, in our study, we aimed to construct the exosome-related prognostic model to reflect the clinical outcomes and immunological status of ovarian cancer patients. By performing multiple bioinformatics analysis at the single-cell and bulk omics, we constructed an exosome-related prognostic model of four genes. To be specific, patients in the high-risk score group showed better clinical outcomes than those with low risk score. Moreover, the risk score was negatively correlated with the activities of immunological characteristics. Then, we chose SERPINB1 as the representative biomarker of the model.

The role of SERPINB1 has been preliminarily investigated, but its role in tumors is bidirectional. In oral cancer, SERPINB1 promotes cell motility and is overexpressed in invasive oral squamous cell carcinoma [68]. However, in hepatocellular carcinoma and prostate cancer, low expression of SERPINB1 accelerates tumor progression and is associated with poor prognosis [69, 70]. In our research, high SERPINB1 expression predicted well prognosis. In addition, SERPINB1 expression was positively correlated with the enrichment scores of immune subpopulations and immune-related signaling pathways. Furthermore, based on the high-resolution exploration, we found that SERPINB1$^+$ tumor cells communicated with the microenvironment subpopulations frequent than SERPINB1$^-$ tumor cells, further explaining the potential reason of shaping an inflamed TME. All the evidence suggests that SERPINB1 may be a tumor suppressor gene in ovarian cancer.

We acknowledge certain limitations of our study. The first relates to the potential biological regulations of SERPINB1 on exosomes in tumor cells. We preliminarily analyzed the potential correlations between SERPINB1 and biological interesting molecules as well as potential biomarkers, and SERPINB1 showed the stronger correlation with biological interesting molecules (Figure S8), indicating its activity on regulating exosomes uptake and release in tumor cells. We do not have relevant experimental platforms to prove the further roles of SERPINB1, but have to admit that this requires further research. In addition, the prognostic value of the established exosome-related prognostic model needs to be further checked in more in-house cohorts.

Conclusions

To sum up, based on multiple bioinformatics analyses for single-cell and bulk omics, we constructed an exosome-related prognostic model of four genes. Further analysis showed that the risk score was negatively correlated with the immune infiltration. To be specific, patients with high-risk score had lower infiltration of immune subpopulations, while those with low-risk score tended to shape the inflamed TME feature. Subsequently, SERPINB1, positively correlated with the favorable OS and negatively with risk score, was chosen as the representative biomarker of the model. Moreover, SERPINB1 was positively correlated with the infiltration of immune subpopulations. Besides, high-resolution analysis found that SERPINB1$^+$ tumor cells communicated with microenvironment cells frequently, further explaining the potential reason for shaping an inflamed TME.

Supplementary Information

The online version contains supplementary material available at https://doi.org/10.1186/s13048-025-01589-3.

Supplementary Material 1

Supplementary Material 2

Acknowledgements
We thank for Dr. Min Yang (Jiangsu Institute of Nuclear Medicine) for her professional comments on our manuscript.

Author contributions
Shaojie Zhao and Liwei Wu designed the study and reviewed the data. Rui Gu, Liping Jiang, Shuqin Dai, Yajie Yue, Shangjin Li, and Shudan Zheng performed bioinformatics analyses. Rui Gu and Liping Jiang drafted the manuscript. All the authors have read, revised, and approved the manuscript.

Funding
This study was funded by Wuxi Medical Development Discipline-Gynecology and Obstetrics (FZXK2021008), Top Talent Support Program for young and middle-aged people of Wuxi Health Committee (HB2023080) and Wuxi Science and Technology Innovation and Entrepreneurship Project (Y20242116).

Data availability
No datasets were generated or analysed during the current study.

Declarations

Ethics approval
Not applicable.

Consent for publication
All authors are consent for publication.

Competing interests
The authors declare no competing interests.

Author details
[1]Department of Obstetrics and Gynecology, Wuxi School of Medicine, Wuxi Maternity and Child Health Care Hospital, Jiangnan University, Jiangsu 214002, China

Received: 26 April 2024 / Accepted: 6 January 2025
Published online: 28 March 2025

References

1. Sung H, Ferlay J, Siegel RL, Laversanne M, Soerjomataram I, Jemal A, et al. Global Cancer statistics 2020: GLOBOCAN estimates of incidence and Mortality Worldwide for 36 cancers in 185 countries. CA Cancer J Clin. 2021;71(3):209–49. https://doi.org/10.3322/caac.21660.
2. Matulonis UA, Sood AK, Fallowfield L, Howitt BE, Sehouli J, Karlan BY. Ovarian cancer. Nat Rev Dis Primers. 2016;2:16061. https://doi.org/10.1038/nrdp.2016.61.

3. Lengyel E. Ovarian cancer development and metastasis. Am J Pathol. 2010;177(3):1053–64. https://doi.org/10.2353/ajpath.2010.100105.
4. Torre LA, Trabert B, DeSantis CE, Miller KD, Samimi G, Runowicz CD, et al. Ovarian cancer statistics, 2018. CA Cancer J Clin. 2018;68(4):284–96. https://doi.org/10.3322/caac.21456.
5. Bookman MA. Optimal primary therapy of ovarian cancer. Ann Oncol. 2016;27(Suppl 1):i58–62. https://doi.org/10.1093/annonc/mdw088.
6. Pujade-Lauraine E, Fujiwara K, Ledermann JA, Oza AM, Kristeleit R, Ray-Coquard IL, et al. Avelumab alone or in combination with chemotherapy versus chemotherapy alone in platinum-resistant or platinum-refractory ovarian cancer (JAVELIN ovarian 200): an open-label, three-arm, randomised, phase 3 study. Lancet Oncol. 2021;22(7):1034–46. https://doi.org/10.1016/S1470-2045(21)00216-3.
7. Xiao Y, Yu D. Tumor microenvironment as a therapeutic target in cancer. Pharmacol Ther. 2021;221:107753. https://doi.org/10.1016/j.pharmthera.2020.107753.
8. Kalluri R, LeBleu VS. The biology, function, and biomedical applications of exosomes. Science. 2020;367(6478). https://doi.org/10.1126/science.aau6977.
9. He C, Zheng S, Luo Y, Wang B. Exosome Theranostics: Biology and Translational Medicine. Theranostics. 2018;8(1):237–55. https://doi.org/10.7150/thno.21945.
10. Ludwig AK, Giebel B. Exosomes: small vesicles participating in intercellular communication. Int J Biochem Cell Biol. 2012;44(1):11–5. https://doi.org/10.1016/j.biocel.2011.10.005.
11. Raimondo S, Saieva L, Corrado C, Fontana S, Flugy A, Rizzo A, et al. Chronic myeloid leukemia-derived exosomes promote tumor growth through an autocrine mechanism. Cell Commun Signal. 2015;13:8. https://doi.org/10.1186/s12964-015-0086-x.
12. Al-Nedawi K, Meehan B, Micallef J, Lhotak V, May L, Guha A, et al. Intercellular transfer of the oncogenic receptor EGFRvIII by microvesicles derived from tumour cells. Nat Cell Biol. 2008;10(5):619–24. https://doi.org/10.1038/ncb1725.
13. Yang Y, Li CW, Chan LC, Wei Y, Hsu JM, Xia W, et al. Exosomal PD-L1 harbors active defense function to suppress T cell killing of breast cancer cells and promote tumor growth. Cell Res. 2018;28(8):862–4. https://doi.org/10.1038/s41422-018-0060-4.
14. Maybruck BT, Pfannenstiel LW, Diaz-Montero M, Gastman BR. Tumor-derived exosomes induce CD8(+) T cell suppressors. J Immunother Cancer. 2017;5(1):65. https://doi.org/10.1186/s40425-017-0269-7.
15. Whiteside TL. Exosomes and tumor-mediated immune suppression. J Clin Invest. 2016;126(4):1216–23. https://doi.org/10.1172/JCI81136.
16. Wolfers J, Lozier A, Raposo G, Regnault A, Thery C, Masurier C, et al. Tumor-derived exosomes are a source of shared tumor rejection antigens for CTL cross-priming. Nat Med. 2001;7(3):297–303. https://doi.org/10.1038/85438.
17. Altieri SL, Khan AN, Tomasi TB. Exosomes from plasmacytoma cells as a tumor vaccine. J Immunother. 2004;27(4):282–8. https://doi.org/10.1097/00002371-200407000-00004.
18. Ning Y, Shen K, Wu Q, Sun X, Bai Y, Xie Y, et al. Tumor exosomes block dendritic cells maturation to decrease the T cell immune response. Immunol Lett. 2018;199:36–43. https://doi.org/10.1016/j.imlet.2018.05.002.
19. Chen IH, Xue L, Hsu CC, Paez JS, Pan L, Andaluz H, et al. Phosphoproteins in extracellular vesicles as candidate markers for breast cancer. Proc Natl Acad Sci U S A. 2017;114(12):3175–80. https://doi.org/10.1073/pnas.1618088114.
20. Keller S, Ridinger J, Rupp AK, Janssen JW, Altevogt P. Body fluid derived exosomes as a novel template for clinical diagnostics. J Transl Med. 2011;9:86. https://doi.org/10.1186/1479-5876-9-86.
21. Melo SA, Luecke LB, Kahlert C, Fernandez AF, Gammon ST, Kaye J, et al. Glypican-1 identifies cancer exosomes and detects early pancreatic cancer. Nature. 2015;523(7559):177–82. https://doi.org/10.1038/nature14581.
22. Yang D, Zhang W, Zhang H, Zhang F, Chen L, Ma L, et al. Progress, opportunity, and perspective on exosome isolation - efforts for efficient exosome-based theranostics. Theranostics. 2020;10(8):3684–707. https://doi.org/10.7150/thno.41580.
23. Lugini L, Matarrese P, Tinari A, Lozupone F, Federici C, Iessi E, et al. Cannibalism of live lymphocytes by human metastatic but not primary melanoma cells. Cancer Res. 2006;66(7):3629–38. https://doi.org/10.1158/0008-5472.CAN-05-3204.
24. Zijlstra C, Stoorvogel W. Prostasomes as a source of diagnostic biomarkers for prostate cancer. J Clin Invest. 2016;126(4):1144–51. https://doi.org/10.1172/JCI81128.
25. Tothill RW, Tinker AV, George J, Brown R, Fox SB, Lade S, et al. Novel molecular subtypes of serous and endometrioid ovarian cancer linked to clinical outcome. Clin Cancer Res. 2008;14(16):5198–208. https://doi.org/10.1158/1078-0432.CCR-08-0196.
26. Bonome T, Levine DA, Shih J, Randonovich M, Pise-Masison CA, Bogomolniy F, et al. A gene signature predicting for survival in suboptimally debulked patients with ovarian cancer. Cancer Res. 2008;68(13):5478–86. https://doi.org/10.1158/0008-5472.CAN-07-6595.
27. Wu J, Zeng D, Zhi S, Ye Z, Qiu W, Huang N, et al. Single-cell analysis of a tumor-derived exosome signature correlates with prognosis and immunotherapy response. J Transl Med. 2021;19(1):381. https://doi.org/10.1186/s12967-021-03053-4.
28. Wang X, Chai Z, Pan G, Hao Y, Li B, Ye T, et al. ExoBCD: a comprehensive database for exosomal biomarker discovery in breast cancer. Brief Bioinform. 2021;22(3). https://doi.org/10.1093/bib/bbaa088.
29. Regner MJ, Wisniewska K, Garcia-Recio S, Thennavan A, Mendez-Giraldez R, Malladi VS et al. A multi-omic single-cell landscape of human gynecologic malignancies. Mol Cell. 2021;81(23):4924-41 e10. https://doi.org/10.1016/j.molcel.2021.10.013
30. Wang X, Miao J, Wang S, Shen R, Zhang S, Tian Y, et al. Single-cell RNA-seq reveals the genesis and heterogeneity of tumor microenvironment in pancreatic undifferentiated carcinoma with osteoclast-like giant-cells. Mol Cancer. 2022;21(1):133. https://doi.org/10.1186/s12943-022-01596-8.
31. Korsunsky I, Millard N, Fan J, Slowikowski K, Zhang F, Wei K, et al. Fast, sensitive and accurate integration of single-cell data with Harmony. Nat Methods. 2019;16(12):1289–96. https://doi.org/10.1038/s41592-019-0619-0.
32. Tsuyuzaki K, Sato H, Sato K, Nikaido I. Benchmarking principal component analysis for large-scale single-cell RNA-sequencing. Genome Biol. 2020;21(1):9. https://doi.org/10.1186/s13059-019-1900-3.
33. Shekhar K, Lapan SW, Whitney IE, Tran NM, Macosko EZ, Kowalczyk M et al. Comprehensive Classification of Retinal Bipolar Neurons by Single-Cell Transcriptomics. Cell. 2016;166(5):1308-23 e30. https://doi.org/10.1016/j.cell.2016.07.054
34. Zhu X, Zhang J, Xu Y, Wang J, Peng X, Li HD. Single-cell clustering based on Shared Nearest Neighbor and Graph Partitioning. Interdiscip Sci. 2020;12(2):117–30. https://doi.org/10.1007/s12539-019-00357-4.
35. Langfelder P, Horvath S. WGCNA: an R package for weighted correlation network analysis. BMC Bioinformatics. 2008;9:559. https://doi.org/10.1186/1471-2105-9-559.
36. Yoshihara K, Shahmoradgoli M, Martinez E, Vegesna R, Kim H, Torres-Garcia W, et al. Inferring tumour purity and stromal and immune cell admixture from expression data. Nat Commun. 2013;4:2612. https://doi.org/10.1038/ncomms3612.
37. Charoentong P, Finotello F, Angelova M, Mayer C, Efremova M, Rieder D, et al. Pan-cancer immunogenomic analyses reveal genotype-immunophenotype relationships and predictors of response to checkpoint blockade. Cell Rep. 2017;18(1):248–62. https://doi.org/10.1016/j.celrep.2016.12.019.
38. Bindea G, Mlecnik B, Tosolini M, Kirilovsky A, Waldner M, Obenauf AC, et al. Spatiotemporal dynamics of intratumoral immune cells reveal the immune landscape in human cancer. Immunity. 2013;39(4):782–95. https://doi.org/10.1016/j.immuni.2013.10.003.
39. Hanzelmann S, Castelo R, Guinney J. BMC Bioinformatics. 2013;14:7. https://doi.org/10.1186/1471-2105-14-7. GSVA: gene set variation analysis for microarray and RNA-seq data.
40. Wu T, Hu E, Xu S, Chen M, Guo P, Dai Z, et al. clusterProfiler 4.0: a universal enrichment tool for interpreting omics data. Innov (Camb). 2021;2(3):100141. https://doi.org/10.1016/j.xinn.2021.100141.
41. The Gene Ontology C. The Gene Ontology Resource: 20 years and still GOing strong. Nucleic Acids Res. 2019;47(D1):D330–8. https://doi.org/10.1093/nar/gky1055.
42. Cai Y, Ji W, Sun C, Xu R, Chen X, Deng Y, et al. Interferon-Induced transmembrane protein 3 shapes an Inflamed Tumor Microenvironment and identifies Immuno-Hot Tumors. Front Immunol. 2021;12:704965. https://doi.org/10.3389/fimmu.2021.704965.
43. Cancer Genome Atlas N. Genomic classification of cutaneous melanoma. Cell. 2015;161(7):1681–96. https://doi.org/10.1016/j.cell.2015.05.044.
44. Shen X, Wang C, Zhu H, Wang Y, Wang X, Cheng X, et al. Exosome-mediated transfer of CD44 from high-metastatic ovarian cancer cells promotes migration and invasion of low-metastatic ovarian cancer cells. J Ovarian Res. 2021;14(1):38. https://doi.org/10.1186/s13048-021-00776-2.
45. Huang Y, Liu Y, Huang Q, Sun S, Ji Z, Huang L, et al. TMT-Based quantitative proteomics analysis of Synovial Fluid-Derived exosomes in Inflammatory Arthritis. Front Immunol. 2022;13:800902. https://doi.org/10.3389/fimmu.2022.800902.

46. Sun H, Wang C, Hu B, Gao X, Zou T, Luo Q, et al. Exosomal S100A4 derived from highly metastatic hepatocellular carcinoma cells promotes metastasis by activating STAT3. Signal Transduct Target Ther. 2021;6(1):187. https://doi.org/10.1038/s41392-021-00579-3.
47. Yang HC, Zhang M, Wu R, Zheng HQ, Zhang LY, Luo J, et al. C-C chemokine receptor type 2-overexpressing exosomes alleviated experimental post-stroke cognitive impairment by enhancing microglia/macrophage M2 polarization. World J Stem Cells. 2020;12(2):152–67. https://doi.org/10.4252/wjsc.v12.i2.152.
48. Lima LG, Ham S, Shin H, Chai EPZ, Lek ESH, Lobb RJ, et al. Tumor microenvironmental cytokines bound to cancer exosomes determine uptake by cytokine receptor-expressing cells and biodistribution. Nat Commun. 2021;12(1):3543. https://doi.org/10.1038/s41467-021-23946-8.
49. Hou X, Yin S, Ren R, Liu S, Yong L, Liu Y, et al. Myeloid-cell-specific IL-6 signaling promotes MicroRNA-223-Enriched Exosome production to Attenuate NAFLD-Associated Fibrosis. Hepatology. 2021;74(1):116–32. https://doi.org/10.1002/hep.31658.
50. Thakur MD, Franz CJ, Brennan L, Brouwer-Visser J, Tam R, Korski K, et al. Immune contexture of paediatric cancers. Eur J Cancer. 2022;170:179–93. https://doi.org/10.1016/j.ejca.2022.03.012.
51. Salcher S, Sturm G, Horvath L, Untergasser G, Kuempers C, Fotakis G, et al. High-resolution single-cell atlas reveals diversity and plasticity of tissue-resident neutrophils in non-small cell lung cancer. Cancer Cell. 2022;40(12):1503–e208. https://doi.org/10.1016/j.ccell.2022.10.008.
52. Zhang Y, Wang XL, Liu JJ, Qian ZY, Pan ZY, Song NP, et al. ICOS/ICOSLG and PD-1 Co-expression is Associated with the progression of colorectal precancerous- carcinoma Immune Microenvironment. J Inflamm Res. 2023;16:977–92. https://doi.org/10.2147/JIR.S401123.
53. Zhang X, Wang Y, Fan J, Chen W, Luan J, Mei X, et al. Blocking CD47 efficiently potentiated therapeutic effects of anti-angiogenic therapy in non-small cell lung cancer. J Immunother Cancer. 2019;7(1):346. https://doi.org/10.1186/s40425-019-0812-9.
54. Catalan R, Orozco-Morales M, Hernandez-Pedro NY, Guijosa A, Colin-Gonzalez AL, Avila-Moreno F, et al. CD47-SIRPalpha Axis as a Biomarker and Therapeutic Target in Cancer: current perspectives and Future challenges in Nonsmall Cell Lung Cancer. J Immunol Res. 2020;2020:9435030. https://doi.org/10.1155/2020/9435030.
55. Yu ZZ, Liu YY, Zhu W, Xiao D, Huang W, Lu SS, et al. ANXA1-derived peptide for targeting PD-L1 degradation inhibits tumor immune evasion in multiple cancers. J Immunother Cancer. 2023;11(3). https://doi.org/10.1136/jitc-2022-006345.
56. Bai F, Zhang P, Fu Y, Chen H, Zhang M, Huang Q, et al. Targeting ANXA1 abrogates Treg-mediated immune suppression in triple-negative breast cancer. J Immunother Cancer. 2020;8(1). https://doi.org/10.1136/jitc-2019-000169.
57. Xiong W, Zhang B, Yu H, Zhu L, Yi L, Jin X. RRM2 regulates sensitivity to Sunitinib and PD-1 blockade in Renal Cancer by stabilizing ANXA1 and activating the AKT pathway. Adv Sci (Weinh). 2021;8(18):e2100881. https://doi.org/10.1002/advs.202100881.
58. Mao W, Cai Y, Chen D, Jiang G, Xu Y, Chen R, et al. Statin shapes inflamed tumor microenvironment and enhances immune checkpoint blockade in non-small cell lung cancer. JCI Insight. 2022. https://doi.org/10.1172/jci.insight.161940.
59. Gajewski TF. The next hurdle in Cancer Immunotherapy: overcoming the Non-t-cell-inflamed Tumor Microenvironment. Semin Oncol. 2015;42(4):663–71. https://doi.org/10.1053/j.seminoncol.2015.05.011.
60. Song Y, Wang M, Tong H, Tan Y, Hu X, Wang K, et al. Plasma exosomes from endometrial cancer patients contain LGALS3BP to promote endometrial cancer progression. Oncogene. 2021;40(3):633–46. https://doi.org/10.1038/s41388-020-01555-x.
61. Demory Beckler M, Higginbotham JN, Franklin JL, Ham AJ, Halvey PJ, Imasuen IE, et al. Proteomic analysis of exosomes from mutant KRAS colon cancer cells identifies intercellular transfer of mutant KRAS. Mol Cell Proteom. 2013;12(2):343–55. https://doi.org/10.1074/mcp.M112.022806.
62. Najaflou M, Shahgolzari M, Khosroushahi AY, Fiering S. Tumor-derived extracellular vesicles in Cancer Immunoediting and their potential as Oncoimmunotherapeutics. Cancers. 2022;15(1). https://doi.org/10.3390/cancers15010082.
63. Dai S, Wan T, Wang B, Zhou X, Xiu F, Chen T, et al. More efficient induction of HLA-A*0201-restricted and carcinoembryonic antigen (CEA)-specific CTL response by immunization with exosomes prepared from heat-stressed CEA-positive tumor cells. Clin Cancer Res. 2005;11(20):7554–63. https://doi.org/10.1158/1078-0432.CCR-05-0810.
64. Filipazzi P, Burdek M, Villa A, Rivoltini L, Huber V. Recent advances on the role of tumor exosomes in immunosuppression and disease progression. Semin Cancer Biol. 2012;22(4):342–9. https://doi.org/10.1016/j.semcancer.2012.02.005.
65. Chalmin F, Ladoire S, Mignot G, Vincent J, Bruchard M, Remy-Martin JP, et al. Membrane-associated Hsp72 from tumor-derived exosomes mediates STAT3-dependent immunosuppressive function of mouse and human myeloid-derived suppressor cells. J Clin Invest. 2010;120(2):457–71. https://doi.org/10.1172/JCI40483.
66. Ridder K, Sevko A, Heide J, Dams M, Rupp AK, Macas J, et al. Extracellular vesicle-mediated transfer of functional RNA in the tumor microenvironment. Oncoimmunology. 2015;4(6):e1008371. https://doi.org/10.1080/2162402X.2015.1008371.
67. Ham S, Lima LG, Chai EPZ, Muller A, Lobb RJ, Krumeich S, et al. Breast Cancer-derived exosomes alter macrophage polarization via gp130/STAT3 signaling. Front Immunol. 2018;9:871. https://doi.org/10.3389/fimmu.2018.00871.
68. Tseng MY, Liu SY, Chen HR, Wu YJ, Chiu CC, Chan PT, et al. Serine protease inhibitor (SERPIN) B1 promotes oral cancer cell motility and is over-expressed in invasive oral squamous cell carcinoma. Oral Oncol. 2009;45(9):771–6. https://doi.org/10.1016/j.oraloncology.2008.11.013.
69. Lerman I, Ma X, Seger C, Maolake A, Garcia-Hernandez ML, Rangel-Moreno J, et al. Epigenetic suppression of SERPINB1 promotes inflammation-mediated prostate Cancer progression. Mol Cancer Res. 2019;17(4):845–59. https://doi.org/10.1158/1541-7786.MCR-18-0638.
70. Cui X, Liu Y, Wan C, Lu C, Cai J, He S, et al. Decreased expression of SERPINB1 correlates with tumor invasion and poor prognosis in hepatocellular carcinoma. J Mol Histol. 2014;45(1):59–68. https://doi.org/10.1007/s10735-013-9529-0.

Publisher's note